Hydrothermal synthesis of compounds in the fresnoite mineral family ($Ba_2TiSi_2O_8$)

Edward E. Abbott, Matthew Mann, Joseph W. Kolis*

Department of Chemistry and Center for Optical Materials Science and Engineering Technologies (COMSET), Clemson University, 485 Hunter Labs, Clemson, SC 29634-0973, USA

ARTICLE INFO

ABSTRACT

Crystals of $Ba_2TiSi_2O_8$, $Sr_2TiSi_2O_8$, and $Ba_2VSi_2O_8$, all belonging to the fresnoite family were prepared by the hydrothermal method. Attempts to synthesize other members by substitution at the alkaline earth site, transition metal site, and tetrahedral site were not successful, but did lead to the formation of a variety of other mineral phases as well as the incommensurate structure, $Ba_2TiGe_2O_8$. Structural studies on this compound and analysis of the other known fresnoite phases were performed to elucidate the nature of the incommensurate structure.

1. Introduction

One interesting aspect of the crystal chemistry of titanates is the tendency for the titanium ion to form a highly distorted octahedron in the solid state [1]. This tendency often lends itself to the formation of polar and acentric materials that have applications in wave-guides, second harmonic generation, piezo-electricity and pyroelectricity [2]. A second interesting aspect of titanates is the nature of the d^0 electronic configuration of the Ti^{4+} ion, which allows for transparency and low temperature luminescence with potential applications as lumiphores [3,4].

One interesting d^0 titanate is the mineral fresnoite ($Ba_2TiSi_2O_8$), which exists as a layered material in the acentric space group of $P4bm$ [5]. $Ba_2TiSi_2O_8$ has been investigated for use as a ferroelectric and as a second harmonic generator (SHG), due to the polarizibility tenser leading to a very high SHG coefficient and strong birefringence [6–11]. However, naturally occurring fresnoite is a rare mineral, difficult to isolate as large single crystals. Synthetic fresnoite is most frequently prepared by ceramic methods or melt techniques at high temperatures (1480 °C) [12]. Despite the interesting physical properties of the fresnoites, single crystals of fresnoite that are grown from high temperature methods often contain defects that limit the quality of physical measurements and its use as a material for optical elements [12]. Furthermore, careful structural investigations suggest that the structure contains some subtle complexity. In that hydrothermal crystal growth is well known for its lower synthesis temperatures and ability to produce crystals of high optical quality [13]; we investigated possible routes to fresnoite and its various derivatives using the hydrothermal growth method. In this paper, we present the results of our investigation into the hydrothermal crystal growth of this family of compounds. We report a suitable growth method of the parent material and several derivatives, as well as some preliminary investigations of their physical and structural properties. In addition, we found that subtle variations in the growth parameters lead to a wide variety of other interesting solid-state products.

2. Experimental

2.1. Hydrothermal synthesis

Reactions were performed using the following reagents as received:

Alfa Aesar: amorphous SiO_2 –325 mesh (99.9%), HfO_2 technical grade, RbOH 50 wt% aqueous solution (99.6+%), CsOH 50 wt% aqueous solution (99%) Strem: $Ba(OH)_2$ reagent grade, MnO_2 (99+%), ZrO_2, Aldrich: NaOH semiconductor grade (99.99%), GeO_2 (99.998%), TiO 30 mesh (99.9%), VO_2 (99.9%), V_2O_5 (98%), and KOH (85+%).

Reactions were performed in silver ampoules made from ¼″ silver tubing (Stern Leach, 99.99%) cut to 2 in lengths. These ampoules were filled with various powders and a mineralizer solution before being welded shut. The sealed ampoules were placed in a 27 ml Rene autoclave with a line seal. This autoclave was filled with water and pressurized with 17 psi of water at room temperature, using a hydraulic pump. Autoclaves were placed in a vertical muffle furnace packed with insulation and heated to reaction

temperatures over the course of several hours, while the pressure was monitored. Pressure in excess of the desired values was bled off during the heating phase. The autoclave was differentially heated to establish a temperature gradient from top to bottom of +50 °C. The size and placement of the ampoules suggest reactions had a considerably smaller effective temperature gradient, although the temperature gradient across an ampoule was not explicitly measured. The autoclave was heated for three days and cooled in air to room temperature over the course of 1–3 h. Ampoules were removed and opened; the contents filtered from the supernatant liquor, and those products were rinsed with copious amounts of water and acetone and allowed to dry.

For a typical synthesis of the parent fresnoite 0.205 mmole of $Ba(OH)_2$, 0.126 mmole of TiO_2 and 0.403 mmole of SiO_2 would be combined in a reaction ampoule with 0.3 ml of 50 wt% aqueous solution of CsOH and heated to 500 °C with a 50° temperature gradient and reacted for five days to form the desired $Ba_2TiSi_2O_8$. The germinate analogue was formed by combination of 0.205 mmole of $Ba(OH)_2$, 0.126 mmole TiO_2, and 0.416 mmole of GeO_2 with 0.3 ml of a 5 M solution of KOH heated for five days at 500 °C with a 50° temperature gradient. The synthesis of $Ba_2VSi_2O_8$ consists of the combination of 0.205 mmole of $Ba(OH)_2$, 0.201 mmole VO_2, and 0.403 mmole of SiO_2 with 0.3 ml of a 5 M solution of KOH heated for five days at 500 °C with a 50° temperature gradient. All other reactions were performed under nearly identical conditions using reaction parameters described in the text.

2.2. Characterization

2.2.1. Single crystal X-ray diffraction

Single crystal analysis was preformed using crystals chosen from the reaction mixtures with minimum dimensions of 0.1 mm on a side and mounting them on a glass fiber using epoxy. Diffraction data was taken either on a Rigaku AFC8 diffractometer equipped with a CCD detector or Nicolet R3mV 4 circle diffractometer, using a graphite monochromated Mo $K\alpha$ ($\lambda = 0.71073$ Å) radiation sources. For data acquired on Rigaku AFC8 system, 600 images were taken with χ and ϕ fixed at 45° and 0°, respectively, while ω scanned between $-90°$ and 90° using 0.3° spacings, and 200 images were taken with χ and ϕ fixed at 45° and 90°, respectively, while ω was scanned between values of $-30°$ and 30° with 0.3° spacings. Image exposure time was varied between 5 and 15 s per frame dependent on crystal size and quality. Refinement of source data uses the *Crystal Clear, Texsan*, and *Shelx* crystal refinement programs [14–16]. X-ray powder diffraction was performed on a Scintag XDS 2000 θ–2θ powder diffractometer, using Cu $K\alpha$ radiation.

2.2.2. ESR and infrared analysis

The ESR spectrum of $Ba_2VSi_2O_8$ was taken from ~2 mg of crystals placed in a quartz ESR tube and analyzed using a Bruker EMX spectrometer with a microwave frequency of 9.859 GHz. Infrared analysis was performed by mixing ground crystals of the analyte with KBr and pressed into pellets at 8000 psi. These pellets were analyzed on Nicolet Magma 550 spectrometer.

3. Results and discussion

3.1. Fresnoite ($Ba_2TiSi_2O_8$) synthesis

It is known that subtle variation of reaction conditions can lead to a plethora of different structural types within a natural hydrothermal growth system [17,18]. This also occurs in the hydrothermal TiO_2–SiO_2–$Ba(OH)_2$ system, forming the various products illustrated in Fig. 1. With minor variations in reactants and mineralizers, we can isolate crystalline products of sanbornite ($BaSi_2O_5$),
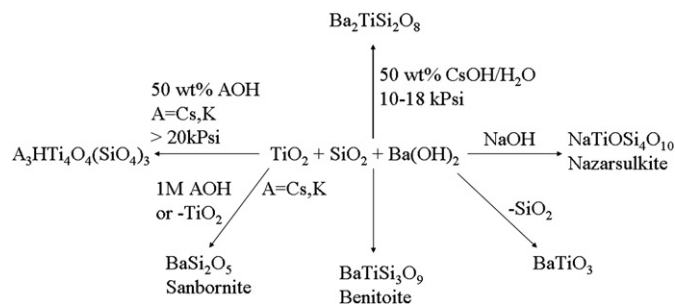

Fig. 1. Synthetic tree for hydrothermal system of TiO_2–SiO_2–$Ba(OH)_2$ at 500 °C.

nazarsulkite ($NaTiOSi_4O_{10}$), perovskite ($BaTiO_3$), benitoite ($BaTiSi_3O_9$), the pharmacosiderite structure ($Cs_3HTi_4O_4(SiO_4)_3$), as well as the target compound, fresnoite ($Ba_2TiSi_2O_8$), were isolated. All reactions presented in the pursuit of the fresnoite structures were performed between 450 and 500 °C for 3–14 days. Reaction length and temperature variations within those prescribed have some effect on crystal quality and size, but isolatable products remain the same, except where noted. There were a variety of reaction conditions employed leading to a complex mixture of products in many cases; however, conditions were developed that lead to good crystals of the target compound, fresnoite.

The suite of products shown in Fig. 1 is not to be unexpected particularly, since sanbornite and benitoite phases often exist in mineralogical samples containing fresnoite [19]. Despite the complex chemistry described herein, suitable hydrothermal route to excellent quality single crystals of fresnoite was developed. The use of alkali hydroxides of Cs and Rb proved to work well as mineralizers for the isolation of fresnoite with minimization of side products when the reaction pressure was kept below ~18 Kpsi. While $Ba(OH)_2$ could serve both as a mineralizer and reactant, the desired product was typically only small crystals or microcrystalline powder. In order to increase the hydroxide mineralizer concentration while maintaining a controlled Ba^{2+} ion concentration, various alkali hydroxides were included in the reaction. Crystal formation was notably improved with the use of 5 M rubidium or cesium hydroxides as a mineralizer in addition to $Ba(OH)_2$. Presumably, decreased solubility of $Ba(OH)_2$ in highly alkaline media is overridden by an increased solubility of TiO_2 and SiO_2 in such basic conditions, with the latter factors as the driving force for an increased crystal growth.

The external pressure on the ampoules is equal to the reaction pressure due to the compressibility of the silver ampoules. Since the less dense pharmacosiderite phase ($P_{calc} = 3.472$) [20] is favored at higher pressure rather than the higher density fresnoite ($P_{calc} = 4.462$), it is our presumption that pressure changes effect the solvent system favoring the chemical speciation in the 'solution' phase that leads to the fresnoite structure at low pressures and the pharmacosiderite phase at high pressures.

Under the best indentified conditions, fresnoite crystallized as long rectangular needles with approximate dimensions of 0.1×0.1 mm and up to 1.0 mm in length in nearly quantitative yield. The infrared spectra of hydrothermally synthesized crystals match the previously reported spectra by Blasse [4]. These crystals also display distinct blue luminescence under UV radiation as has been reported for the previously grown synthetic samples in contrast to the yellow luminescence of naturally occurring samples [4,19]. These crystals were of sufficient quality to provide a satisfactory single crystal structure shown in Table 1.

3.2. Substitution of the parent fresnoite structure

Derivatization of the parent fresnoite structure was systematically attempted at the titanium metal site with V, Zr, Mn, and Hf

Table 1
Crystallographic data for $Ba_2TiGe_2O_7$, $Ba_2TiSi_2O_8$, $Ba_2VSi_2O_8$, and $Ba_2TiGe_2O_8$.

Chemical formula	$Ba_2TiSi_2O_8$	$Ba_2VSi_2O_8$	$Ba_2TiGe_2O_8^*$
Diffractometer	Rigaku AFC8	Nicolet P3mV	Rigaku AFC8
Formula weight (g/mol)	506.69	509.80	595.76
$a(\text{Å})$	8.521(12)	8.5060(10)	8.6693(12)
$c(\text{Å})$	5.195(10)	5.2304(1)	5.3167(11)
$V(\text{Å}^3),Z$	377.2(1), 2	378.4(1), 2	402.97(1), 2
Space group	$P4bm$	$P4bm$	$P4$
P_{calc}	4.462	4.474	4.910
Crystal shape	Square needles	Square pyramids	Rectangular block
Crystal color	Colorless	Green	Colorless
Size (mm)	$0.1 \times 0.1 \times 0.5$	$0.2 \times 0.2 \times 0.2$	$0.15 \times 0.15 \times 0.5$
Indices (min)	$[-10, -10 -6]$	$[0, -10 -6]$	$[-10, -10 -6]$
(max)	$[10, 10, 6]$	$[10, 10, 6]$	$[10, 10, 6]$
Number of reflections Measured $I > 2\sigma$	3212	1286	3867
Number of reflections Unique (R_{int})	411, 0.0623	376, 0.0623	818, 0.1888
Number of parameters	38	39	46
Final R(F), wR^2	0.0341, 0.0614	0.0285, 0.0699	0.0612, 0.2000
Goodness of fit (S)	1.175	1.139	1.159
Residual ($e^-/\text{Å}^{-3}$) maximum shift	0.048/0.014	1.473/0.038	1.544/0.035

Table 2
Hydrothermal exploratory reactions.

Reactants	Mineralizer	Days	Products
$2Ba(OH)_2 + VO_2 + 2SiO_2$	5 M KOH	5	$Ba_2VSi_2O_8$
$2Sr(OH)_2 + TiO_2 + 2SiO_2$	AOH (A=Rb, Cs) 50 wt/wt%	6	$A_2TiSi_3O_9$ (major) $Sr_2TiSi_2O_8$ (minor)
$2Ba(OH)_2 + TiO_2 + 2GeO_2$	AOH (A=K,Rb,Cs) 50 wt/wt%	5	$Ba_2TiGe_2O_8$
$2Ba(OH)_2 + TiO_2 + xTiO + 2GeO_2$ $x < 0.25$	AOH (A=Cs) 50 wt/wt%	4	$Ba_2TiGe_2O_8$ (major) $Ba_2TiGe_2O_7$ (minor)
$Ba(OH)_2 + TiO_2 + TiO + 2GeO_2$	KOH 50 wt/wt%	7	$Ba_2TiGe_2O_8$ (major) $K_2TiO_5 \cdot H_2O$ (minor)
$2Ba(OH)_2 + TiO_2 + TiO + 2GeO_2$	KOH 50 wt/wt%	14	$K_2Ti_4O_8(OH)_2$
$2Ba(OH)_2 + TiO_2 + 2VO_2$	KOH 50 wt/wt%	5	$TiVO_4$
$2Ba(OH)_2 + TiO_2 + 2HfO_2$	5 M CsOH	4	$BaHfO_3$

All reactions performed at 500 °C.

Fig. 2. An ESR spectrum of $Ba_2VSi_2O_8$.

substitution. Likewise, exchange of the barium site with Sr substitution also occurred, as silicon was replaced with germanium. Of these substitutions, hydrothermally grown crystals of $Ba_2VSi_2O_8$, $Sr_2TiSi_2O_8$, and $Ba_2TiGe_2O_8$ were isolated in the fresnoite family. Analogous conditions to those used for $Ba_2TiSi_2O_8$ were used as a starting point for the substitution synthesis with the full details presented in Table 2.

$Ba_2VSi_2O_8$ was first isolated by crystallization from a melt by Feltz and co-workers [21]. While the crystal structure was inferred from powder data, a structure using single crystal diffraction was not presented until Höche [22]. The structure of $Ba_2VSi_2O_8$ contains isolated vanadyl groups as one-dimensional chains along the c-axis separated by SiO_4^{-2} tetrahedra. Synthesis of this fresnoite phase was isolated at 500 °C by substituting VO_2 for TiO_2 in the traditional fresnoite synthesis scheme shown in Fig. 1. A change in the mineralizer solution to 5 M KOH facilitated crystal growth of $Ba_2VSi_2O_8$, rather than RbOH and CsOH utilized in the growth of $Ba_2TiSi_2O_8$. The dark green crystals obtained from this reaction had approximate dimensions of 0.25 mm per side and display a square pyramidal morphology. The single crystal structure data for this compound is presented in Table 1, indicating that it is isostructural with fresnoite. The presence of a single electron on the square pyramidal V^{4+} ion can be clearly seen in the ESR spectrum, as displayed in Fig. 2. This is similar to the isotropic signature in the compound
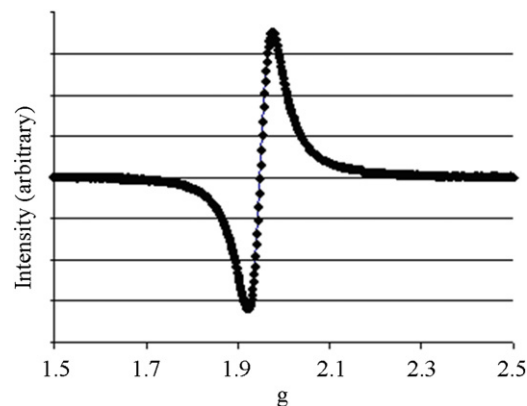
$VOHPO_4 \cdot 0.5H_2O$, which has V^{4+} in the square pyramidal geometry [23]. The g value of 1.94 for the compound is close to the isotopic g values for other V^{4+} compounds $VOSO_4 \cdot 2H_2O$ (1.96), $VOSO_4 \cdot 5H_2O$ (1.99), and $VOCl_2$ (2.00) [24].

$Sr_2TiSi_2O_8$, the strontium analog to the parent compound [25–27] displays a decreased propensity for hydrothermal growth than $Ba_2TiSi_2O_8$. Nevertheless, a low yield ($\sim$10%) of small crystals can be isolated as a side product from a reaction of $Sr(OH)_2$, TiO_2, and SiO_2 at 500 °C in CsOH and RbOH mineralizer solutions. The primary products in these reactions were identified as a series of wadeite analogs, $A_2TiSi_3O_9$ (A=Rb, Cs) [28]. $Sr_2TiSi_2O_8$ grown hydrothermally displays distinct yellow luminescence under UV radiation and thus can be readily separated from $A_2TiSi_3O_9$ (A=Rb, Cs).

Crystals of the germinate analog, $Ba_2TiGe_2O_8$, can be grown in AOH (A=K, Rb, Cs) mineralizers by substituting GeO_2 for SiO_2. $Ba_2TiGe_2O_8$ forms as large ($\sim$0.3 $\times$ 0.3 $\times$ 1.25 mm) colorless rectangular columns in a good yield and display a yellow luminescence when viewed under a UV radiation source. Unfortunately, these crystals often display single needle like domains in the center of the bulk crystal similar to striations reported from Bridgeman melt growth [29]. Thus, the structure of $Ba_2TiGe_2O_8$ grown hydrothermally could not be well solved in spite of the apparently high quality of crystals. This phenomenon will be discussed in the following section.

In an attempt to obtain better quality crystals of $Ba_2TiGe_2O_8$, a variety of different reagents were evaluated. When a small amount of TiO is added to a typical fresnoite synthesis in CsOH solutions, a new product, $Ba_2TiGe_2O_7$, was isolated as a minor product. $Ba_2TiGe_2O_7$ is a new compound and is a member of a series of transition metal germinates with the formula $A_2BGe_2O_7$, where A=Ba/Sr and B=Mn, Zn, Cu, Co that belongs to the melilite mineral family [30]. This species forms as blue cubes coincident with the growth of $Ba_2TiGe_2O_8$. This chemistry will be the subject of a subsequent paper.

The chemistry of this system was investigated over a wide array of stoichiometries of $TiO:TiO_2$, with the crystallinity of products suffering greatly if the $TiO:TiO_2$ ratio exceeds 0.25:1. If equivalent amounts of titanium oxides (Table 2) are used, a different set of products emerges. This reaction leads to the formation of the fresnoite derivative $Ba_2TiGe_2O_8$ and a kinetically stable product $K_2Ti_2O_5 \cdot H_2O$ over a one-week reaction time. If the reaction is allowed to proceed for a two week span, the products listed above are subsequently consumed, and $K_2Ti_4O_8(OH)_2$ is formed as the only detectable microcrystalline product.

Several other substitutions of the fresnoite structure were briefly investigated. It is known that mixed-valent vanadium can replace silicate in $Rb_2V_3O_8$ with a similar structure [31]. The

combination of TiO_2 and VO_2 (Table 2) leads to the formation of small black crystals of the compound $TiVO_4$ with a disordered rutile structure [32] rather than the possible $Ba_2TiV_2O_8$ fresnoite analogue. Also attempted was the substitution of zirconium for titanium in a variety of reactions to prepare a zirconium fresnoite analogue. However, no successful formation of any fresnoite analogues was detected with either germinate or silicate anion. Rather $ZrGeO_4$ or $ZrSiO_4$ crystallized as the favored products. Efforts to form pure manganese derivatives of fresnoite directly were unsuccessful, so MnO_2 was added to reactions in the alkaline hydrothermal TiO_2–$Ba(OH)_2$–SiO_2 system in attempts to isolate a manganese derivative as a possible product (Fig. 1). Introduction of small amounts of MnO_2 in reactions did lead to the formation of manganese doped orange crystalline analogues of benitoite ($BaTiSi_3O_9$) and the pharmacosiderite analogue ($Cs_3HTi_4O_4(SiO_4)_3$). Unfortunately, fresnoite showed no such tendency towards manganese doping and no minority products were detected either. The subsequent chemistry of these materials was not investigated further.

Attempts to use HfO_2 rather than TiO_2 in CsOH solutions resulted in the formation of a microcrystalline powder of the perovskite $BaHfO_3$. While the preparation of $BaHfO_3$ is well known [33], and a patent for the low temperature hydrothermal synthesis of $BaHfO_3$ has recently been issued [34], this reaction provides a new route to highly crystalline $BaHfO_3$.

3.3. Fresnoite structural analysis

The structure of fresnoite was originally presented by Moore and Louisnathan on a naturally occurring sample of indifferent quality [5,35]. The structure of $Ba_2TiSi_2O_8$, and its family members, has three main structural motifs: a five coordinate titanium site exhibiting square pyramidal geometry, a four coordinate silicon site exhibiting tetrahedral geometry, and a 10 coordinate barium site with significant variations in bond lengths exhibiting roughly pentagonal antiprismatic geometry. Fresnoite exhibits a layered structure with layers formed from the tetrahedra and square pyramids separated by the alkali or alkali earth metal residing in the center of the 10 coordinate site. The layers of the square pyramids and tetrahedra are formed with bases of these two motifs residing roughly in plane with the remaining oxygen atoms protruding perpendicular to the plane. Given the highly polar nature of the structure, it is not surprising that such high non-linear optical coefficients were reported [9]. A view along the polar c-axis has been provided (Fig. 3).

The crystal structure of $Ba_2TiGe_2O_8$ has been reported in the past as belonging to the space groups $Cmm2$ and $Iba2$, as well as the parent $P4bm$ [29,36]. The orthorhombic cells represent super-cell refinements of the parent structure with slight distortions that lead to a reduction in symmetry in the overall structure. Recent reports by Höche, Withers, et al. reveal that the structure of $Ba_2TiGe_2O_8$ is actually an incommensurate structure, elucidated by the use of electron diffraction and tunneling electron microscopy [22,26,37]. A primary motivation of this work is to determine if the reported incommensurate structure was actually due to the high growth temperature or is inherent to the material. Thus, a detailed structural solution was refined on a hydrothermally grown sample.

While hydrothermally prepared $Ba_2TiSi_2O_8$ was accurately refined in this work, this was not achieved with the germanium analog. Crystal structure solutions attempted from hydrothermally grown crystals refined in the possible space groups $Ccc2$, $P4$, and $P4bm$ display variance in the thermal parameters with non-definite oxygen placement of atoms about the GeO_4^{-2} tetrahedra. These observations are in keeping with the reported distortions in those
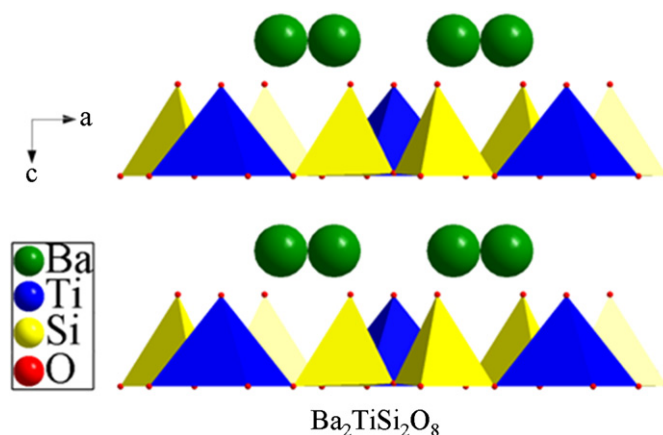

Fig. 3. The polar axis of $Ba_2TiSi_2O_8$.

materials grown from high temperature methods that lead to the various super cell refinements ($Cmm2$ and $Iba2$) [38,39]. Refinement attempts were made on many crystals at both room temperature and at low temperature ($-100\,^\circ C$). Structural refinement was also attempted using several models under a space group of reduced symmetry, $P4$. Initially the refinement allowed the non-bridging oxygen atoms in the corner-shared germinate Ge_2O_7 dumbbell to be disordered, while the germanium atoms and the bridging oxygen atom were rigidly held in place. This model did not lead to a satisfactory structural refinement. Further attempts used a refinement of a model in which the GeO_4 tetrahedra in the Ge_2O_7 dumbbells were allowed to be disordered, while the GeO_4 group was rigidly defined as a tetrahedra with only the bridging oxygen atoms rigidly held in place (on their special position in the $P4$ space group). Unfortunately this approach also did not lead to a satisfactory refinement. Lastly, this system was modeled as a possible twin of right and left handed chiral layers with the chirality arising from the symmetric displacement of GeO_4 tetrahedra about the transition metal square pyramid that resides co-incident with the four-fold rotation axis, again leading to no satisfactory refinement. Thus, while related to the parent fresnoite crystal structure, $Ba_2TiGe_2O_8$ is not truly isostructural with it. Similarly, $Ba_2TiGe_2O_8$ cannot be described simply as a disordered fresnoite structure. It seems to follow that the hydrothermally prepared samples exhibit the same incommensurate structure observed in those crystals prepared by melt techniques [22,26].

The analogous incommensurately modulated structures of $Ba_2TiGe_2O_8$ have been suggested to exist for each member of the fresnoite family that have been investigated for such structural features by electron diffraction and powder neutron diffraction experiments. The incommensurate nature of the structure is suggested to be a function of the bonding of the 10 fold coordinated atom [36].

If one views the distortion in this structure with focus on the regularity of the pentangular arrangement, resulting from the five-membered ring of oxygen atoms formed by two transition metal square pyramids and three corner sharing tetrahedra that sit in plane (Figs. 4 and 5), may suggest other reasons for the instability in these fresnoite structures. The five atoms that are roughly in plane form an approximate pentagram. While the angles associated with the square pyramids and tetrahedra are such that this pentagram cannot be regular (where all angles are ideally 108°), the oxygen atoms will have an energy minimum when evenly spaced. Considering the Shannon radii for the various elements and the corresponding geometric constraints for ideal tetrahedra and square pyramids, those fresnoite structures that have minimal deviation in the oxygen–oxygen distances along edges of this base pentangle
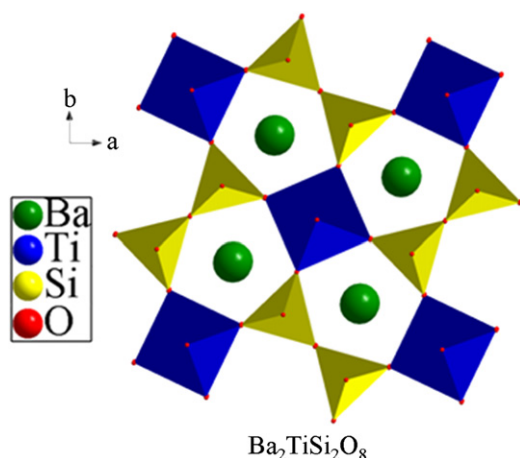
Fig. 4. *c*-Axis projection of $Ba_2TiSi_2O_8$ grown hydrothermally showing the pentagonal arrangement of oxygens, which form half of the 10 fold coordination environment of the barium atoms.
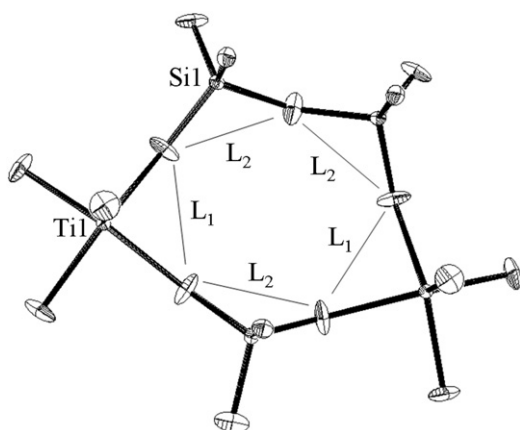

Fig. 5. A view of the $Ba_2TiSi_2O_8$ pentagram with 50% displacement ellipsoids.

Table 3
Theoretical O–O distances in the pentagram outlined in Fig. 4.

Structure	$L1$ (Å)	$L2$ (Å)	Mean of L	Standard deviation of L
$K_2TiP_2O_8$	2.547	2.531	2.537	0.009
$K_2MnSi_2O_7Cl$	2.643	2.645	2.644	0.001
$Ba_2VSi_2O_8$	2.574	2.645	2.617	0.039
$Ba_2TiSi_2O_8$	2.547	2.645	2.606	0.054
$Rb_2V_3O_8$	2.574	2.833	2.730	0.142
$Ba_2VGe_2O_8$	2.574	2.890	2.764	0.173
$Ba_2TiGe_2O_8$	2.547	2.890	2.753	0.188

Table 4
Bond valence sums of the 10 fold coordination site.

Compound	Ion	Bond valence sum
$Ba_2TiSi_2O_8$	Ba^{2+}	1.94
$Ba_2VSi_2O_8$	Ba^{2+}	1.90
$Ba_2TiGe_2O_8$	Ba^{2+}	1.79
$Ba_2MnSi_2O_7Cl$	Ba^{2+}	1.82
$Sr_2TiSi_2O_8$	Sr^{2+}	1.53
$Rb_2V_3O_8$	Rb^+	1.07
$K_2V_3O_8$	K+	1.02

Bond valence sum calculations [47,48].

seem to be the most stable. Thus, structures of the parent $Ba_2TiSi_2O_8$ and $Ba_2VSi_2O_8$ have significantly more regular spacing of these oxygen atoms as shown in Table 3. This feature may account for the higher quality of the structural solution for these compounds. The previously reported fresnoite family compounds $Ba_2TiGe_2O_8$, $A_2V_3O_8$ ($A=K^+$, NH_4^+, Rb^+) [a fresnoite $A_2V^{(4+)}V_2^{(5+)}O_8$] [31,40], the disordered $(NH_4)_2V^{(4+)}V^{(5+)}_{(2-x)}P_xO_8$ [41], and the potential $Ba_2VGe_2O_8$ structure display significant variance in this parameter due to a mismatch in the square pyramid and tetrahedron size. This suggests that $Ba_2TiGe_2O_8$ and $Ba_2VGe_2O_8$ are structures with considerable strain arising from the size mismatch of the germinate tetrahedra and the transition metal square pyramid manifesting itself in the highly incommensurate structure of $Ba_2TiGe_2O_8$ and the $Ba_2VGe_2O_8$ structure, which has not been isolated.

Some other known fresnoite type members, including $BaKCuV_2O_7Cl$ [42], $K_2MnSi_2O_7Cl$ [43], and the related structure $K_4Nb_2Si_4O_{14}$ [44] have considerably lower variance in the regularity of the spacing of these oxygen atoms, leading to stable structures in high symmetry of compositionally complex compounds. The compound $Cs_2TiP_2O_8$ looks like a potential fresnoite analog and would have a very regular five-membered ring, but the small size of this ring is likely too small to accommodate the large monovalent Cs^+ ion, and thus this structure adopts a different structure with a seven-membered ring about the Cs^+ ion in the space group $P2_12_12_1$ [45]. In

contrast, the related compound $K_2VP_2O_8$ with the smaller K^+ ion does display the fresnoite structure [46].

According to Höche, the compounds of $Ba_2VSi_2O_8$, $Ba_2TiSi_2O_8$ have first order modulations, while the compound $Sr_2TiSi_2O_8$ displayed second order satellite reflections, but could still be modeled as a first order modulation while the compound $Ba_2TiGe_2O_8$ displays significant higher order modulations [27]. This is in keeping with the geometric stability of the five-membered ring. The competition between the stability of the static structure and the under bonding of the 10 fold site may be the driving force for the harmonic distortions (Tables 3 and 4).

Analysis for incommensurate structures of other known fresnoite structures would be of interest, particularly those of $K_2VP_2O_8$ with its high degree of regularity and the lack of significant underbonding of the monovalent ion. Additionally, analysis of $A_2V_3O_8$ ($A=K^+$, Rb^+), with its low stability ring displaying a monovalent ion that has limited underbonding could serve as comparison between structures. Given the many possible combinations of 5 fold coordinate metals and tetrahedral structural constituents, there exists a large number of undiscovered fresnoite analogs, particularly in regards to the transition metal silicates and phosphates.

4. Conclusion

Hydrothermal synthesis provides a low temperature route to the synthesis of single crystals of multiple members of the fresnoite family. The crystals of $Ba_2TiGe_2O_8$ prepared at the relatively low hydrothermal temperatures displayed the same incommensurate structure as those prepared from the high temperature melt. Thus, we conclude that this feature of $Ba_2TiGe_2O_8$ is inherent to the structure rather than due to high temperature effects generated during the melt crystal growth. We propose that the stability of the fresnoite structure depends on the relative sizes of the square pyramid and tetrahedra structural motifs. Further study into the incommensurate structure of the lesser-investigated members of fresnoite family of compounds would further likely elucidate the structural and physical properties of the fresnoite structure type. A variety of other mineral phases were isolated from the various chemical variations

explored in this investigation. These include bentioites, pharmacositerites and a new melilite derivative, $Ba_2TiGe_2O_7$.

References

[1] M. Kunz, I.D. Brown, J. Solid State Chem. 115 (1995) 395–406.
[2] P.S. Halasyamani, K.P. Poeppelmeirer, Chem. Mater. 10 (1998) 2753–2769.
[3] G. Blasse, Struct. Bonding 42 (1980) 1–41.
[4] G. Blasse, J. Nucl. Inorg. Chem. 41 (1979) 639–641.
[5] P.B. Moore, J. Louisnathan, Science 156 (1967) 1361–1362.
[6] M.C. Foster, D.J. Arbogast, R.M. Nielson, P. Photinos, S.C. Abrahams, J. Appl. Phys. 85 (1999) 2299–2303.
[7] K. Wu, C.J. Chen, J. Cryst. Growth 166 (1996) 533–536.
[8] K. Masakazu, Y. Fujino, T. Kawamura, Appl. Phys. Lett. 29 (1976) 227–228.
[9] J. Gopalakrishnan, K. Ramesha, K.R. Kasthuri, S. Pandey, J. Solid State Chem. 148 (1999) 75–80.
[10] S.C. Abrahams, Acta Crystallogr. A50 (1994) 658–685.
[11] S.C. Abrahams, Acta Crystallogr. B52 (1996) 790–805.
[12] S. Haussuehl, J. Eckstein, K. Recker, F. Wallrafen, J. Cryst. Growth 40 (1977) 200–204.
[13] R.A. Laudise, R, C&E News, September 28 (1987) 30–43.
[14] Crystal Clear mercury CCD automated imaging system. Version 1.3 Rigaku Corporation, Oren UT (2001).
[15] Texsan single crystal structure analysis software. Version. 1.6b, Molecular Structure Corporation, Woodlands, TX (1993).
[16] G.M. Sheldrick, SHELXTL, Version 6.1 Structure Determination Software Programs, Bruker Analytical X-ray Systems Inc., Madison, 2001.
[17] A.I. Bortun, L.N. Bortun, A. Clearfield, Chem. Mater. 9 (1997) 1854–1864.
[18] K. Lii, Y. Huang, V. Zima, C. Huang, H. Lin, Y. Jiang, F. Liao, S. Wang, Chem. Mater. 10 (1998) 2599–2609.
[19] J. Anthony, K. Bideaux, K. Bladh, M. Nichols, Handbook of Minerology. v.2, Mineral Data Publishing, Tuscon, AZ, 1985 270.
[20] W.T.A. Harrison, T.E. Gier, G.D. Stucky, Zeolites 15 (1995) 408–412.
[21] A. Feltz, S. Schmalfuss, H. Langbein, M. Tietz, Z. Anorg. Allg. Chem. 417 (1975) 125–129.
[22] T. Höche, S. Esmaeilzadeh, R.L. Withers, H. Schirmer, Z. Kristallogr. 218 (2003) 788–794.
[23] A. Bruecker, B. Kubias, B. Lucke, Catal. Today 32 (1996) 215–222.
[24] S.A. Al'tschuler, B.M. Kozyrev, Electron Paramagnetic Resonance, Academic Press, New York NY, 1964 120.
[25] J. Yuan, P. Fu, J. Wang, F. Guo, Z. Yang, Y. Wu, Prog. Cryst. Growth Charact. Mater. 40 (2000) 103–106.
[26] T. Höche, C. Russel, W. Neumann, Solid State Commun. 110 (1999) 651–656.
[27] T. Höche, W. Neumann, S. Esmaeilzadeh, R. Uecker, M. Lentzen, C. Russel, J. Solid State Chem. 166 (2002) 15–23.
[28] J. Choisnet, A. Deschanvres, B. Raveau, J. Solid State Chem. 7 (1973) 408–417.
[29] M. Kimura, K. Doi, S. Nanamatsu, T. Kawamura, Appl. Phys. Lett. 23 (1973) 531–532.
[30] J.V. Smith, Am. Mineral. 38 (1953) 643–661.
[31] M. Linh, H. Eierdanz, U. Müller, Z. Anorg., Allg. Chem. 613 (1992) 63–66.
[32] L.W. Vernon, W.O. Milligan, Tex. J. Sci. 1 (1951) 82–85.
[33] V.R. Scholder, D. Rade, H. Schwartz, Z. Anorg. Allg. Chem. 362 (1968) 149–168.
[34] S.E. Kim, Repub. Korean Kongkae Taeho Kongbo (Korean Patent). KR 2001005146A (2001).
[35] P.B. Moore, S.J. Louisnathan, Z. Kristallogr. 130 (1969) 438–448.
[36] S.A. Markgraf, A. Bhalla, Phase Trans. 18 (1989) 55–76.
[37] R.L. Withers, Y. Tabira, Y. Liu, T. Hoeche, Phys. Chem. Miner. 29 (2002) 624–632.
[38] T. Hoeche, S. Esmaeilzadeh, R. Uecker, S. Lidin, W. Neumann, Acta Crystallogr. B59 (2003) 209–216.
[39] M. Kimura, K. Utsumi, S. Nanamatsu, J. Appl. Phys. 47 (1976) 2249–2251.
[40] G. Liu, J.E. Greedan, J. Solid State Chem. 114 (1995) 499–505.
[41] C. Ninclaus, R. Retoux, D. Riou, G. Ferey, J. Solid State Chem. 122 (1996) 139–142.
[42] F.D. Martin, H. Muller-Bushbaum, Z. Naturforsch. 49b (1994) 355–359.
[43] X. Mo, S.J. Hwu, Inorg. Chem. 42 (2003) 3978–3980.
[44] M.P. Crosnier, D. Guyomard, A. Verbaere, Y. Piffard, M. Tournoux, J. Solid State Chem. 98 (1992) 128–132.
[45] J. Protas, B. Menaert, G. Marnier, B. Boulanger, Acta Crystallogr. C47 (1991) 698–701.
[46] Y.E. Gorbonova, S.A. Linde, A.V. Lavrov, I.V. Tananev, Dokl. Akad. Nauk SSSR 250 (2) (1980) 350–353.
[47] D. Altermatt, I.D. Brown, Acta Crystallogr. B41 (1985) 240–244.
[48] I.D. Brown, D. Altermatt, Acta Crystallogr. B41 (1985) 244–247.